Coupled photorefractive spatial-soliton pairs

Zhigang Chen and Mordechai Segev

Department of Electrical Engineering and Center for Photonics and Optoelectronic Materials, Princeton University, Princeton, New Jersey 08544

Tamer H. Coskun and Demetrios N. Christodoulides

Department of Electrical Engineering and Computer Science, Lehigh University, Bethlehem, Pennsylvania 18015

Yuri S. Kivshar

Optical Sciences Centre, Research School of Physical Sciences and Engineering, Australian National University, ACT 0200 Canberra, Australia

Received April 30, 1997

We provide a comprehensive experimental and theoretical study of incoherently coupled photorefractive spatial-soliton pairs in all three possible realizations: bright–bright, dark–dark, and dark–bright. We also show that when the total intensity of two coupled solitons is much lower than the effective dark irradiance, the coupled soliton pair is reduced to Manakov solitons. In all cases, mutual trapping of both components in the coupled soliton pair is verified by analyzing, experimentally and numerically, the beam evolution after decoupling. © 1997 Optical Society of America [S0740-3224(97)02111-5]

1. INTRODUCTION

Self-trapping of light and formation of optical spatial solitons has been studied since 1964.[1] It has recently attracted considerable interest following the progress on photorefractive solitons,[2] quadratic (or $\chi^{(2)}$) solitons,[3] and solitons in saturable nonlinear media.[4] In addition, since spatial solitons are potentially useful for all-optical switching, three-dimensional optical interconnects,[5] and waveguide applications,[6,7] research in this field has spanned from soliton formation to soliton-induced waveguides to soliton interactions. The purpose of this paper is to provide a comprehensive study of incoherently coupled photorefractive spatial-soliton pairs.

Soliton pairing has been studied previously in the spatiotemporal domain (in Kerr media) by employing two coupled nonlinear Schrödinger equations. In particular, it has been shown that an optical pulse can propagate undistorted in a single-mode fiber as a bright soliton when it couples to a dark soliton (at a different wavelength) through cross-phase modulation[8–10] (XPM). Pairing of bright and/or dark fundamental temporal solitons corresponds to a particular set of solutions of the coupled nonlinear wave equations.[8–10] These studies were then extended to the spatial domain, where the evolution of spatial solitons in Kerr media is governed by the same set of nonlinear Schrödinger equations, similar to the spatiotemporal analogy discussed for the scalar solitons.[11] It has been shown theoretically that pairing of bright and/or dark spatial solitons of two different wavelengths can be realized in a self-focusing or defocusing Kerr-type medium through XPM, provided that the two soliton components have properly scaled relative intensities when they are superimposed.[12] Indeed, a coupled bright–dark spatial-soliton pair has been observed experimentally in a focusing Kerr medium with two beams of different colors.[13]

Pairing of two spatial solitons has always been an intriguing issue among spatial-soliton interactions. Specifically, in the case of a coupled soliton pair the two beams are mutually trapped and depend on each other in such a way that each of them propagates undistorted. The presence of both components is required, since each beam alone cannot survive as a soliton if the other beam is absent. On the other hand, it is well known that a spatial soliton forms a self-induced waveguide that can guide not only the soliton beam itself but also another probe beam.[14] Extending this concept to the nonlinear case, we come to a coupled soliton pair, for which the refractive-index modulation (or the self-induced waveguide) is created by the two pairing beams and both beams are self-guided, whereas in guiding a beam in a soliton-induced waveguide the index modulation is set only by the soliton that remains unchanged if the guided beam is removed. Thus a coupled soliton pair is in contradistinction to guiding a probe beam in a soliton-induced waveguide.

In general, two copropagating beams in a nonlinear medium are known to interact through XPM. Thus, removing one beam should affect the other since the XPM term disappears. For a coupled soliton pair, which consists of two soliton components of nearly equal amplitude, the XPM is comparable with the self-phase modulation (SPM) of each beam, and both effects play an important role in forming a coupled soliton pair. Therefore, when one beam is absent, the other cannot remain as a soliton. On the other hand, for a weak beam guided in a soliton-induced waveguide, the XPM is small enough relative to

0740-3224/97/113066-12$10.00

the SPM (one beam has a higher intensity than the other) that the weak beam does not greatly affect the strong beam. At the same time the weak beam is guided in the waveguide induced by the strong beam (provided that the strong beam alone can form a soliton). In this latter case, even though the weak beam by itself is not a soliton, it is guided by the strong beam through XPM. When the weak beam is removed, the strong one still remains a soliton. In fact, this is why the guided beam must be much weaker than the soliton beam itself in all experiments with Kerr spatial solitons. Because of this subtlety, the nomenclature of coupled soliton pairs or soliton pairing is in general used for the case that two beams are mutually self-trapped and coupled to form solitons simultaneously, as has been used previously.[12,13]

In this paper we present an experimental and a theoretical study of coupled photorefractive spatial-soliton pairs. Photorefractive solitons were predicted a few years ago,[2] and they have been studied extensively since then. Photorefractive solitons exhibit several interesting properties that are different from Kerr-type solitons. For instance, these solitons are stable in both transverse dimensions and can be generated even at microwatt power levels.[15] Also unique to photorefractive solitons is that a weak soliton beam can induce a waveguide that can guide in it an intense beam of a wavelength that is photorefractively less sensitive.[16] Thus far, photorefractive solitons have been observed in biased photorefractive crystals in both quasi steady state[2,15,17,18] and steady state,[5,19–27] in photovoltaic media[28–32] as well as in photorefractive semiconductors.[33] It has also been shown that even a spatially incoherent optical beam can be self-trapped by use of the photorefractive nonlinearity.[34,35] Among these studies, of particular interest are the steady-state photorefractive solitons, which use the effect of nonuniform screening of the externally applied electric field and are thus called screening solitons.[19] When an optical beam passes through a properly biased photorefractive crystal, the refractive-index change resulting from the nonuniformly screened electric field can have a self-focusing or a defocusing effect on the beam, depending on the polarity of the applied field with respect to the crystalline axes.[5,19,20] Both bright[22–24] and dark[25–27] screening solitons can be obtained once the self-focusing or -defocusing effect balances diffraction. Since the first prediction[19] of screening solitons, attention has also been drawn to their induced waveguides[25,26,36] and their coherent and incoherent interactions.[37–46]

There are three different initial configurations in which two one-dimensional spatial solitons can interact in the same plane: overlapping, parallel propagating, and crossing. When two coherent fundamental photorefractive screening solitons are launched close to each other (parallel propagating but not overlapping), interaction between them leads to their attraction or repulsion, depending on their initial phase difference,[45,47,48] similar to the interaction of two Kerr-type spatial solitons.[49] Interaction between two one-dimensional incoherent colliding screening solitons has been studied in Ref. 42.

Here we investigate the interaction between two incoherent overlapping (copropagating) photorefractive screening solitons that leads to coupled spatial-soliton pairs. As predicted in Ref. 37, an incoherently coupled photorefractive soliton pair can be generated if two mutually incoherent optical beams copropagate in a biased photorefractive crystal and experience the same refractive index and electro-optic coefficient. Experimentally, a possible choice is to use two beams of approximately the same wavelength and polarization that are at the same time mutually incoherent. This means that the interference pattern between these two beams must fluctuate randomly with time much faster than the response time of the photorefractive medium. The formation time of photorefractive screening solitons is roughly given by the dielectric relaxation time, τ_{die}, which is longer than 1 ms in all photorefractive nonsemiconductor crystals for an optical illumination of $\sim 1\ \mathrm{W/cm^2}$ maximum intensity. This implies that for such two beams to form an incoherent soliton pair, their average frequencies must be different by $\Delta\nu \gg 1/\tau_{\mathrm{die}} \approx 1$ kHz. If one uses both beams from the same laser source and delays them with respect to one another, then the coherence length of the laser, l_c, must be much shorter than $c\,\tau_{\mathrm{die}} \approx 100$ km (c is the speed of light in vacuum). On the other hand, each component of the soliton pair must maintain its own coherence throughout propagation, which implies that l_c must be much longer than the propagation length in the nonlinear medium (approximately a few centimeters). Therefore we find it convenient to work with a multimode argon-ion laser of $l_c \approx 10$ cm [$l_{\mathrm{xtal}} \ll l_c \ll c\,\tau_{\mathrm{die}}$] and to delay the two beams by ~ 3 m with respect to each other so that they are mutually incoherent from the perspective of the nonlinear medium. Thus the two pairing beams have roughly the same wavelength. In addition, both beams are extraordinarily polarized in order to use the optimal electro-optic coefficients for soliton formation in the photorefractive crystal[5,19,20] (note that both beams now experience the same reflective index and electro-optic coefficient) so that the two pairing beams also have the same polarization. Because of the mutual incoherence, the two beams are now coupled merely through nonlinear intensity-driven XPM. When such two beams propagate collinearly in a biased photorefractive crystal, they can couple to form a steady-state screening-soliton pair under certain conditions. In Ref. 37, coupled soliton-pair solutions (bright–bright, dark–dark, or dark–bright) have been found at a particular set of parameters for two beams that have identical full width at half-maximum (FWHM) but different peak intensities. As we show in the present paper, if the intensity difference between two beams is too large, they resemble a coupled soliton pair, but the two beams have a master–slave relation that is close to the case of guiding one beam by the other.

The paper is organized as follows: In Sections 2 and 3 we present a theoretical model for the study of coupled photorefractive soliton pairs and an intuitive understanding of such soliton pairs from the existence curve of the photorefractive screening solitons. The Manakov soliton limit is discussed in Section 4. In Section 5 we discuss the experimental setup and the technique used to separate and characterize the two beams from a coupled pair (despite their having the same frequency and polarization). Sections 6–8 deal with three different configurations of soliton pairing, namely, bright–bright, dark–

dark, and dark–bright. Both experimental results and numerical simulations of coupled soliton propagation are presented. It is shown that, while a coupled bright–bright or dark–dark photorefractive soliton pair propagates like a single fundamental bright or dark screening soliton, a dark–bright soliton pair corresponds to self-guided propagation of both beams. Furthermore, we discuss the coupling–decoupling behavior of a soliton pair (i.e., two beams can couple to form a soliton pair, but one beam alone cannot preserve the soliton behavior without the other). In Section 9 we discuss some other issues such as the stability of coupled soliton pairs. Conclusions are given in Section 10.

2. MODEL

For photorefractive screening solitons the theoretical model that characterizes the evolution of one-dimensional spatial solitons in biased photorefractive media is now well established[5,19,20] and has been tested experimentally.[24,25] The basic equations are the Helmholtz equation for the slowly varying amplitude of the optical field and a set of the charge-transport equations that describe the photorefractive effect in a nonlinear medium. These equations reduce to a single nonlinear equation and can be extended to the case of two optical beams copropagating in a photorefractive medium. In steady state the coupled wave equations can be written as

$$\left[\frac{\partial}{\partial z} - \frac{i}{2k}\frac{\partial^2}{\partial x^2} - \frac{ik}{n_b}\Delta n(E_{sc})\right]\Phi(x, z) = 0,$$

$$\left[\frac{\partial}{\partial z} - \frac{i}{2k}\frac{\partial^2}{\partial x^2} - \frac{ik}{n_b}\Delta n(E_{sc})\right]\Psi(x, z) = 0, \qquad (1)$$

where $\Phi(x, z)$ and $\Psi(x, z)$ are the slowly varying amplitudes of the two optical fields, x and z are the transverse and longitudinal coordinates, respectively, $k = 2\pi n_b/\lambda$, n_b is the unperturbed index of refraction, and λ is the free-space wavelength. $\Delta n(E_{sc})$ is the change in the refractive index, which is driven by the space-charge field $E_{sc}(x, z)$ through the electro-optic effect

$$\Delta n(E_{sc}) = -\frac{1}{2} n_b{}^3 r_{33} E_{sc}. \qquad (2)$$

In writing Eqs. (1) and (2), we assume that the two beams copropagate in the z direction with the same wavelength λ and the same polarization. When the photorefractive crystal is strontium barium niobate (SBN), the most favorable configuration for soliton formation is when the crystalline c axis is parallel to the x direction, which is also the direction of beam polarization, and employs the large electro-optic coefficient r_{33}. Under appropriate conditions the steady-state space-charge field is approximately given by[5,19,20]

$$E_{sc} = E_0 \frac{I_\infty + I_d}{I(x, z) + I_d}, \qquad (3)$$

where E_0 is the space-charge field at $x \to \pm\infty$, and it is approximately equal to $\pm V/l$, that is, the voltage V applied across the crystal of width l. $I(x, z)$ is the total intensity of the two optical beams. $I_\infty = I(x \to \pm\infty)$ represents the total intensity far away from the center of the beams (near the crystal x boundaries), and I_d is the effective dark irradiance.[5,19,20] (When no background beam is provided for dark illumination, I_d is just the natural dark irradiance in the crystal. When a background illumination is provided and is much stronger than the natural dark irradiance, I_d is roughly the intensity of the background beam). For two mutually incoherent beams the total intensity can be considered as the sum of the two Poynting fluxes, i.e., $I = (n_e/2\eta_0)(|\Phi|^2 + |\Psi|^2)$, where $\eta_0 = (\mu_0/\epsilon_0)^{1/2}$. It is through this intensity superposition that the two beams are coupled, since the total optical intensity modifies the space-charge field through Eq. (3) and thus modifies the refractive-index of the crystal through Eq. (2). The refractive-index change induced by both beams is then experienced by each beam through Eqs. (1). Under appropriate normalization of $\zeta = z/(kx_0{}^2)$, $\xi = x/x_0$, $\Phi = (2\eta_0 I_d/n_b)U$, and $\Psi = (2\eta_0 I_d/n_b)V$, Eqs. (1) can be written as two coupled nonlinear equations in dimensionless variables[37]:

$$i\frac{\partial U}{\partial \zeta} + \frac{1}{2}\frac{\partial^2 U}{\partial \xi^2} - \beta(1 + \rho)\frac{U}{1 + |U|^2 + |V|^2} = 0,$$

$$i\frac{\partial V}{\partial \zeta} + \frac{1}{2}\frac{\partial^2 V}{\partial \xi^2} - \beta(1 + \rho)\frac{V}{1 + |U|^2 + |V|^2} = 0, \qquad (4)$$

where $\rho = I_\infty/I_d$, $\beta = 1/2(kx_0)^2 n_b{}^2 r_{33} E_0$, and x_0 is an arbitrary spatial width for scaling. These are the basic equations we used in our theoretical modeling.

3. SOLITON SOLUTIONS AND THE EXISTENCE CURVES

In general, Eqs. (4) are not integrable, and therefore their spatially localized solutions of any kind should be found only numerically by separation of the trajectories of the corresponding stationary problem. However, because the saturable nonlinearity depends on the total intensity ratio, Eqs. (4) have a family of the solitary-wave solutions of equal width but unequal amplitudes that can be obtained from the theory of single-beam propagation in a photorefractive medium. To see this, we discuss each case individually. For the case of bright–bright soliton pairs the intensities are expected to vanish at the boundaries ($\xi \to \pm\infty$); thus we have $I_\infty = \rho = 0$. To seek such soliton-pair solutions, we can express the normalized envelopes U and V as $U = r^{1/2} y(\xi)\cos\theta \exp(i\mu\zeta)$ and $V = r^{1/2} y(\xi)\sin\theta \exp(i\mu\zeta)$, where r is the total peak intensity of the pair normalized to the effective dark irradiance [$r = I_0/I_d$, and $I_0 = I(\xi = 0)$ is the total peak intensity of this bright two-component beam configuration], $y(\xi)$ is a normalized real function bounded between $0 \leqslant y(\xi) \leqslant 1$, θ is an arbitrary projection angle, and μ represents a nonlinear shift of the propagation constant.[37] Then Eqs. (4) can be reduced to

$$\frac{d^2 y}{d\xi^2} - 2\mu y - \frac{2\beta}{1 + r y^2} y = 0. \qquad (5)$$

This equation is known to allow bright solitons when β or E_0 is positive, which corresponds to a negative sign of $\Delta n(\xi)$ for all ξ, and a net self-focusing effect on the optical

beam. The bright-soliton solutions of Eq. (5) have been discussed in great detail,[5,19,20] and these studies have predicted a unique relation for the soliton width, the applied field, and the intensity ratio I_0/I_d, i.e., the ratio of the peak soliton intensity to the sum of the natural dark irradiance and the uniform background illumination. This relation constitutes the soliton existence curve shown in Fig. 1(a), where we plot the soliton width in normalized units $\Delta\xi = \Delta x k n_e (r_{33} V/l)^{1/2}$ (Δx is the soliton FWHM in actual units) as a function of the square root of the peak intensity ratio. The existence curve for bright solitons has been verified in several experiments.[24,39,45] In our case of coupled soliton pairs the two components can be considered as the θ projections of the fundamental bright-soliton envelope. We note that these are only the simplest type of solutions in which $|U|^2$ and $|V|^2$ have the *same* functional dependence on ξ.

Dark–dark soliton pairs can be analyzed in a similar way. A one-dimensional dark spatial soliton is a dark notch resulting from an antisymmetric field profile that remains invariant while propagating in a nonlinear medium. Thus I_∞ and ρ are now nonzero quantities [$\rho = I_\infty/I_d$, and $I_\infty = I(\xi \to \pm\infty)$ is the peak intensity for dark beams]. The envelopes of the two dark (notch-bearing) beams can then be expressed as $U = \rho^{1/2} y(\xi) \times \cos\theta \exp(i\mu\zeta)$ and $V = \rho^{1/2} y(\xi) \sin\theta \exp(i\mu\zeta)$, where $|y(\xi)| \leqslant 1$. Equations (4) now become

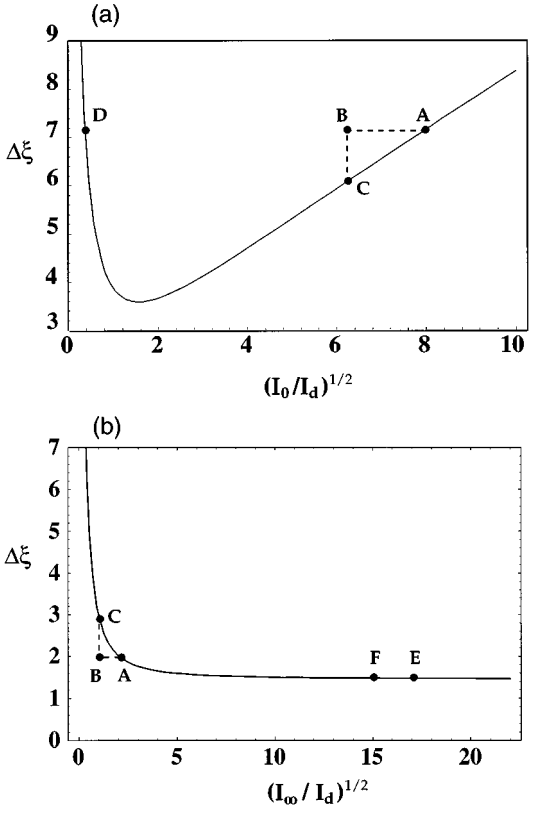

Fig. 1. Theoretical plot of the existence curves (normalized soliton width versus the square root of the intensity ratio) for fundamental (a) bright and (b) dark photorefractive solitons. The points marked by filled circles correspond to conditions discussed in the text.

$$\frac{d^2 y}{d\xi^2} - 2\mu y - \frac{2\beta(1+\rho)}{1+\rho y^2}\, y = 0. \tag{6}$$

This equation is known to allow dark solitons when β or E_0 is negative, which corresponds to a positive sign of $\Delta n(\xi)$ for all ξ, and a net self-defocusing effect on the notch-bearing optical beams. The dark-soliton solutions of Eq. (6) have been studied extensively,[5,19,20] and the soliton existence curve for dark solitons has been found [see Fig. 1(b)] to be quite different from the one for bright solitons in the high-intensity regime ($I_\infty/I_d \gg 1$). The existence curve has also been verified experimentally.[25] Again, the two components of a dark–dark pair can be simply obtained through a θ projection.

Intuitively, one can understand coupled soliton pairs from the photorefractive soliton existence curves of Fig. 1. As observed in many experiments,[23–27,39] a large deviation of the experimental parameters from a soliton existence curve proves unfavorable for soliton propagation. For instance, an optical beam diffracts if the applied voltage is not high enough (at a particular intensity ratio), and it is distorted by instabilities[24,39] or, for a broad input dark notch, breaks up into multiple filaments[26,27] if the voltage is too high. Both the applied voltage and the intensity ratio control the nonlinearity, as seen from Eqs. (2) and (3). For the case of a bright–bright soliton pair, two mutually incoherent beams of the same size can form a coupled soliton pair as long as their combined intensity ratio and width match the curve of Fig. 1(a). However, once they are decoupled (i.e., one beam is blocked), each beam alone cannot remain as a soliton under the same experimental conditions. For instance, if the coupled soliton pair is formed from two identical bright beams at certain bias field and intensity ratio that corresponds to point A on the existence curve of Fig. 1(a), blocking one beam shifts the operating point to B since now the intensity ratio is reduced by half. This in turn entails a large deviation from the curve, and thus each component by itself can no longer behave like a soliton. In fact, the nonlinearity becomes too high for self-trapping of a single beam at this bias field, which may lead to beam breakup into filaments. A bright soliton can be retrieved either by decreasing the bias field that moves the operating point to C or by readjusting the intensity ratio that moves the operating point to A or D.

Similarly, a dark–dark photorefractive soliton pair can be obtained, provided that their total intensity ratio and normalized width match the curve of Fig. 1(b). Because the existence curve for dark solitons is different from that for bright, the behavior of each beam after decoupling is also different. If a coupled dark–dark pair is formed in the region of low intensity ratio, e.g., at point A on the curve of Fig. 1(b) ($I_\infty/I_d \leqslant 10$), blocking one beam shifts the operating point to B as the intensity ratio is reduced. Now a large deviation from the curve leads to diffraction of the dark notch (rather than breakup), since the nonlinearity is not high enough at this bias field for each beam to form a dark soliton, unless the bias is increased to match point C. However, if a coupled pair is formed in the region of high intensity ratio, say, at point E on the curve of Fig. 1(b) ($I_\infty/I_d \gg 1$), blocking one beam shifts the operating point to F, which still roughly matches the

curve, because the existence curve is practically flat for $I_\infty \gg I_d$, and reducing I_∞ by half does not change $\Delta\xi$. In this case, no significant change is expected when a dark–dark soliton pair is decoupled. Thus for dark–dark pairs, significant difference after decoupling is only expected for I_∞/I_d well below 10.

Finally, a dark–bright soliton pair solution can also be obtained from the coupled equations [Eqs. (4)] under proper conditions.[37] When the peak intensity of a bright beam I_0 and that of a dark beam I_∞ are comparable but not equal, the combined intensity pattern can be of a bright peak (when $I_0 > I_\infty$) or a dark notch (when $I_0 < I_\infty$) in the center of the beam; thus it is equivalent to either a bright or a dark beam that will require different polarity of the bias field for soliton formation. Interestingly, a stable dark–bright photorefractive pair can be realized only with a self-defocusing nonlinearity when the combined intensity pattern is of a dark notch, i.e., when $I_0 < I_\infty$. This dark notch can be self-trapped at an appropriate negative bias, similar to ordinary dark (or gray) photorefractive screening solitons. When the bright component is blocked, the effective intensity ratio is increased.[41] As a result, the nonlinearity is too high to support a fundamental dark soliton of the same width. If the applied field is not adjusted accordingly, the dark notch evolves into multiple dark solitons when the input notch is broad enough or breaks up owing to transverse instabilities if the input notch is too narrow.[27] From Fig. 1(b), this corresponds to moving point A somewhere to the right, and thus, in contradistinction to the dark–dark case, it shifts above the curve and the nonlinearity becomes higher. If the total intensity exhibits a bright peak ($I_0 > I_\infty$), then a positive bias is needed to create a self-guided channel for both beams. But, since a bright soliton requires a self-focusing nonlinearity,[5] the bias field leads to modulation instability of the broad background associated with the dark beam. Eventually, no stable dark–bright pair with $I_0 > I_\infty$ can form, no matter where the operating point is on Fig. 1(a). Therefore a dark–bright photorefractive soliton pair requires $I_0 < I_\infty$ and a self-defocusing nonlinearity.

4. MANAKOV SOLITON LIMIT

For the particular case of low total intensity ratio ($|U|^2 + |V|^2 \ll 1$) we can expand the term describing the saturable nonlinearity (as done in Ref. 5) and obtain the following equations:

$$i\frac{\partial u}{\partial \zeta} + \frac{1}{2}\frac{\partial^2 u}{\partial \xi^2} \pm (|u|^2 + |v|^2)u = 0,$$

$$i\frac{\partial v}{\partial \zeta} + \frac{1}{2}\frac{\partial^2 v}{\partial \xi^2} \pm (|u|^2 + |v|^2)v = 0, \tag{7}$$

where the normalized envelopes $u(\zeta, \xi)$ and $v(\zeta, \xi)$ are introduced according to the relations $(U, V) = (u, v) \times [|\beta|(1 + \rho)]^{-1/2} \{\exp[-i\beta(1 + \rho)\zeta]\}$, and the dual sign $\pm$ defines the polarity of the bias field corresponding to focusing or defocusing nonlinearity, respectively.

The system of Eqs. (7) is known as the Manakov equations, and its integrability for the focusing case was established in Ref. 50. It is well known that the localized bright–bright soliton solutions with equal widths but different amplitudes, which can be obtained by a simple reduction of $u(\zeta, \xi) = f(\zeta, \xi)\cos\theta$ and $v(\zeta, \xi) = f(\zeta, \xi)\sin\theta$ (where θ is constant as in Section 3), are the only possible type of one-soliton solutions of the Manakov model, and their common envelope f is described by the cubic nonlinear Schrödinger equation.

As has been shown recently,[51] special polarization properties of the beam propagation in semiconductor AlGaAs planar waveguides allow the TE and TM soliton polarization components of a bright–bright vector soliton to have equal width. This happens when the ratio between the SPM to XPM equals to unity, and the SPM terms must be identical for the two polarization components. The authors of Ref. 51 associated the property of the equal width of the polarization components with those of the Manakov solitons analyzed in Ref. 50. As can be seen from the analysis presented above, the same property is valid for any kind of incoherent soliton interaction, and it is a simple consequence of the dependence of the refractive-index change on the total beam intensity.

The case of defocusing nonlinearity in the Manakov equations did not get enough attention in the past; preliminary study has been started only recently,[52,53] and the dark–dark and dark–bright solitons and their elastic interaction, corresponding to the limit of integrable Manakov model, have been revealed. In this respect, the present paper also reports the first experimental observation of a coupled dark–dark Manakov soliton pair. For the dark–bright case the general solution of Eqs. (7) is

$$u(\zeta, \xi) = \tanh(a\xi)\exp(-i\zeta),$$

$$v(\zeta, \xi) = \sqrt{1 - a^2}\,\mathrm{sech}(a\xi)\exp[-i(1 - a^2/2)\zeta], \tag{8}$$

where the parameter a characterizes the amplitude of the bright component, $0 < a^2 < 1$, provided the total background intensity is normalized to unity (a particular case of this solution was found in Ref. 37). As follows from this exact solution, for any a it describes only a dark notch for the total intensity profile. Because the Manakov model is exactly integrable, it allows the exact solution that describes interaction of any number of solitons. This property does not persist for larger intensity ratios ($|U|^2 + |V|^2 \gg 1$) when the approximation by the Manakov model is not valid, and therefore some new types of generalized Manakov-like solitons are expected.

5. EXPERIMENTAL ARRANGEMENT

The experiments are performed with a cw argon-ion laser and a photorefractive SBN crystal (Fig. 2). The laser beam is collimated and split by a polarizing beam splitter. The ordinarily polarized beam is used as the uniform background illumination so as to mimic the dark irradiance,[22,24,25] whereas the extraordinarily polarized beam is split into two soliton-forming beams. We make these two beams mutually incoherent at the input face of the crystal by having their optical path difference greatly exceed the coherence length of the laser. Thus no stationary interference gratings can form within a time scale

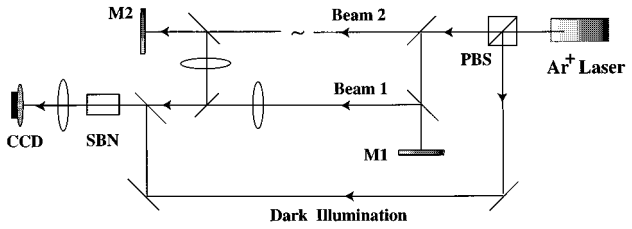

Fig. 2. Experimental setup. Beams 1 and 2 are two soliton-forming beams made incoherent to each other. For bright-beam generation they are cylindrically focused directly onto the crystal input face. For dark-beam generation they are reflected from λ/2 step mirrors (M1 and M2) and then imaged onto the crystal input face.

comparable with the response time of the crystal, as discussed in Section 1. For the bright–bright pair experiments the two bright beams are cylindrically focused (narrow in x and almost uniform in y, which define the transverse plane) onto the crystal input face and are superimposed on each other so that they propagate collinearly through the crystal along the longitudinal direction z. For the dark–dark pair experiments each beam falls on a λ/4 step mirror, which generates upon reflection a narrow dark notch in each beam.[25] The dark notches are then imaged onto the input face of the crystal, with each dark (notch-bearing) beam covering the entire input face of the crystal to ensure steady-state soliton formation.[19,25,27] We vary the width (FWHM) of each beam at the input face of the crystal by using different magnifications of the imaging system and/or by adjusting the variable slit positioned in the central focal plane of the imaging lens. We perform experiments on dark–bright pairs by replacing one of the dark beams by a bright beam and superimposing the bright beam onto the dark notch. In each case, we generate one-dimensional screening solitons by applying an appropriate (in terms of magnitude and polarity) dc field parallel to the crystalline c axis. The input–output beams from the crystal are monitored by a CCD camera.

Since the two collinear beams have roughly the same λ and polarization, it is difficult to distinguish them by use of a λ filter or a polarizer. However, since the space-charge field builds up (or decays) with a response time determined by the dielectric relaxation time τ_{die} (typically a few seconds in our experiments at a beam intensity of $\sim$100 mW/cm^2), a photorefractive soliton and its induced waveguide, once formed, has a memory time of a few seconds. Thus we identify each beam at the coupled output by blocking one beam with a mechanical shutter and sampling the other within a time interval much shorter than τ_{die}. This permits viewing of each soliton beam separately although the two beams share roughly the same frequency and polarization, as the refractive-index modulation (or the soliton-induced waveguide) created by both soliton beams remains unaffected by the rapid change in the intensity within such a short time interval.

6. BRIGHT–BRIGHT PAIRS

The experiments with bright–bright soliton pairs are performed in a 5-mm-long Co-doped SBN:61 crystal. Two bright beams are made to have nearly the same input size (FWHM: 9 μm, $\pm 1\,\mu$m) and nearly the same peak intensity of $\sim$120 mW/cm^2. Without the external field each beam diffracts to $\sim 52\,\mu$m after 5-mm propagation. When both beams are on, the peak intensity ratio I_0/I_d (the ratio between the total peak intensity of the two bright beams and the intensity of the background beam for dark illumination, as defined above) is measured to be 84 with $\sim$20% error. The error is because the beams are not exactly uniform in y; i.e., they are cylindrically focused Gaussian beams rather than ideal one-dimensional beams. By applying a positive voltage of $V = 2150$ V between $l = 4.5$ mm, the output beams are trapped to form a steady-state coupled bright–bright soliton pair. Typical experimental results are presented in Fig. 3, where photographs are taken at the input and output faces of the crystal to show input beams [Fig. 3(a)], output beams of normal diffraction [Fig. 3(b)], and output beams of a coupled soliton pair [Fig. 3(c)]. The photographs of Fig. 3(c) are taken from each beam immediately (less than 0.1 s) after its pairing beam is turned off. We observe that both beams are trapped to their initial input size. The coupled soliton pair corresponds to point A on the soliton existence curve of Fig. 1(a). When the two beams are decoupled, i.e., when one of the two beams is blocked long enough ($t \gg \tau_{\mathrm{die}}$) for the crystal to reach a new steady state, while no other experimental condition is changed, the remaining beam can no longer preserve its soliton properties. Instead, it is severely distorted in the transverse plane because of transverse modulation instability[24]; meanwhile, it exhibits strong self-bending[23,54] toward the crystalline c axis (the latter feature is attributed to the enhanced effect of the diffusion field at high bias[55]). Eventually, the beam breaks up. Figure 3(d) shows the photographs of each beam taken after its pairing beam is blocked for a time (5 min), much longer than the crystal response time. Although

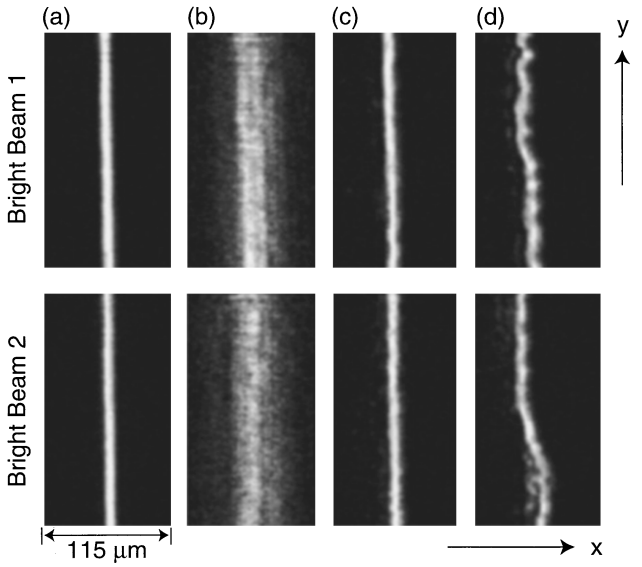

Fig. 3. Experimental results showing coupling–decoupling of a bright–bright soliton pair. Photographs are taken at (a) the input and (b)–(d) the output faces of the crystal: (b) diffraction output from the crystal, (c) coupled output when the pairing beam is present, and (d) decoupled output when the pairing beam is absent.

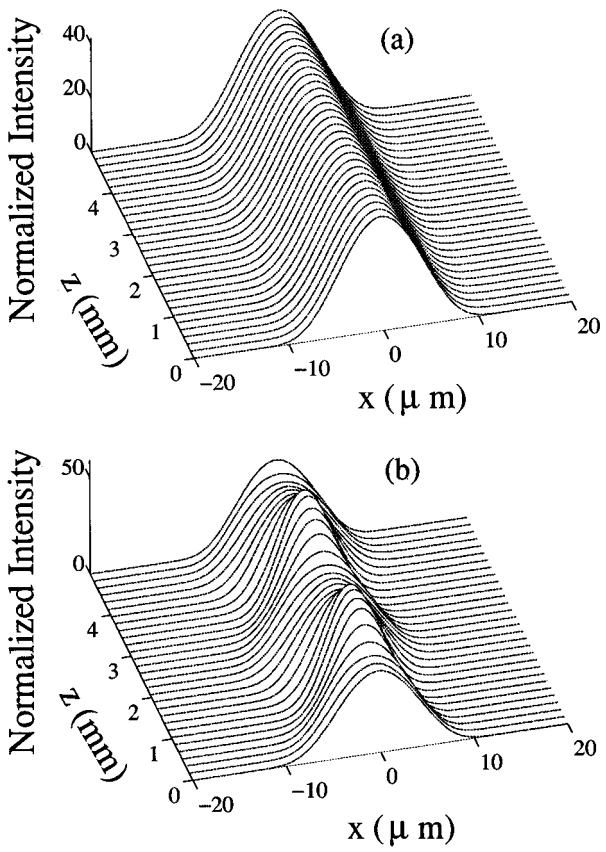

Fig. 4. Numerical simulations corresponding to Figs. 3(c) and 3(d): (a) propagation of one of the bright beams from a coupled bright–bright soliton pair and (b) propagation of one of the bright beams when the pairing beam is absent.

each beam is still focused to a certain degree, it is no longer a soliton, as each beam is highly distorted by transverse instability. From the soliton existence curve of Fig. 1(a), the transition from a coupled pair to the case of one beam alone shifts the operating point from A to B. This implies that the applied voltage of 2150 V is too high for the remaining beam to form a soliton on its own. However, by readjustment of the applied voltage down to 1200 V (without a change in its intensity), each beam alone can then be trapped to form a fundamental soliton. This corresponds to point C in Fig. 1(a).

Numerical simulations are performed to compare with the above experimental observations. The two coupled evolution equations [Eqs. (4)] are solved by beam propagation methods. For simplicity, beam self-bending effects[54,55] are neglected in all our simulations in this paper. (Self-bending was included in our numerical simulations in a previous paper on bright–bright soliton pairs.[39]) The parameters used correspond to those of the experiments: the input FWHM of each beam is 9.9 μm, the positive trapping voltage is 2150 V (over 4.5 mm), and the total intensity ratio is 84, where the two input beams are of equal intensity. The r_{33} electro-optic coefficient of the SBN crystal is 280 pm/V, as measured from experiments. Figure 4(a) depicts each component of such a soliton pair under these conditions. The pair propagates smoothly with a constant shape. When one of the beams is turned off (for the same voltage), each beam does not maintain a constant width while propagating; instead, it experiences considerable oscillation in its width, as illustrated in Fig. 4(b).

We also studied the case that the two bright beams are not identical, e.g., they are different in intensity and/or size. When two beams are of different sizes but with the same intensity, they can still exhibit mutual self-trapping.[39] When the two beams are of different intensities such that one beam is much stronger than the other, they resemble a coupled soliton pair. However, the two beams have a master–slave relation: The weak beam is guided (slaved) in the waveguide dominated (mastered) by the strong beam, as is further discussed in Section 9.

7. DARK–DARK PAIRS

The experiments with dark–dark pairs are performed in a 11.7-mm-long undoped SBN:61 crystal. The r_{33} measured for this crystal is ~247 pm/V. As discussed above on the existence curve for dark solitons [Fig. 1(b)], blocking one beam reduces the total intensity ratio and moves the operating point to the left and below the curve. Thus we should see the diffraction of the dark notch since the nonlinearity is now insufficient to balance diffraction. However, the diffraction of a dark notch (borne on a broad background beam) is smaller than that of a cylindrically focused Gaussian beam of the same size.[27] Therefore we use a longer crystal for observing the decoupling behavior of a dark–dark soliton pair. Two dark notches are now made to have roughly the same input size (FWHM: 16 μm, ± 1 μm), borne on two broad beams of nearly the same average intensity. The two dark notches overlap and propagate collinearly through the crystal. Without the external field, each notch diffracts to ~36 μm. Since the combined intensity pattern is of a deeper dark notch (same FWHM, double intensity of the bearing beam), a negative bias is required to turn the medium into a self-defocusing type for dark-soliton formation.

Indeed, as we set the total intensity of the dark beams less than, or comparable with, the effective dark irradiance (i.e., $I_\infty/I_d \leq 1$, in the region of low intensity ratio), we observe that the two beams are coupled to form a dark–dark screening soliton pair by applying a negative voltage. Typical experimental results are presented in Fig. 5. At $I_\infty/I_d = 0.8$ and $V = -420$ V (applied between $l = 5.3$ mm), the FWHM of each dark soliton is ~14 μm. Again, the photographs of Fig. 5(c) are taken from each beam immediately after its pairing beam is turned off, and those of Fig. 5(d) are taken after the pairing beam is blocked and a new steady state is reached. When both beams are on, they couple to form a soliton pair. However, when one of them is turned off, the other cannot be sustained as a dark soliton, and it broadens to ~24 μm. From Fig. 1(b) the decoupling of the coupled soliton pair corresponds to a transition of the operating point from A to B. This implies that the applied voltage is not high enough for the remaining beam to form a dark soliton on its own. Experimentally, we cannot retrieve the dark soliton just by increasing the applied voltage to match point C because of the strong transverse modulation of the dark beam at high bias field.

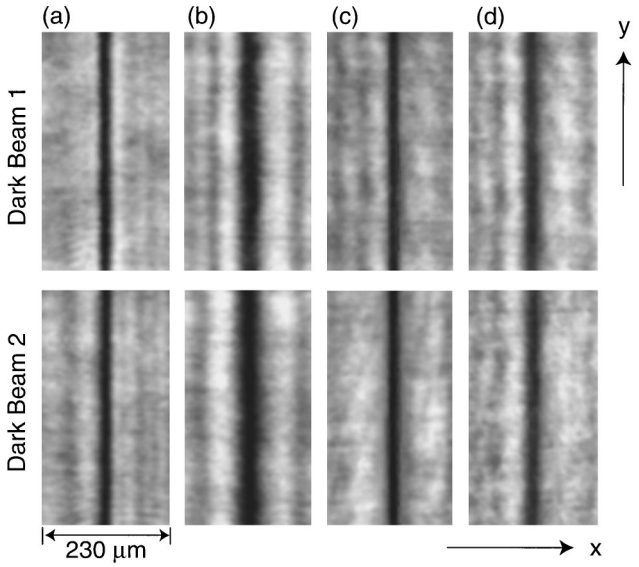

Fig. 5. Experimental results showing coupling–decoupling of a dark–dark soliton pair obtained in the region of low intensity ratio. Photographs are taken at (a) the input and (b)–(d) the output faces of the crystal: (b) diffraction output from the crystal, (c) coupled output when the pairing beam is present, and (d) decoupled output when the pairing beam is absent.

Numerical simulations by beam propagation methods for coupling-decoupling of a dark–dark soliton pair are presented in Fig. 6, where Fig. 6(a) depicts each dark component from a coupled soliton pair, Fig. 6(c) shows the same component after the pairing component is removed, and Fig. 6(c) is the input (solid curve) and output (dashed curve) intensity profiles corresponding to Fig. 6(b). The parameters used for these figures are as follows: the FWHM of each dark notch is 16 μm (which diffracts to 38 μm after propagating through the crystal), the negative trapping voltage is -199.3 V (over 5.3 mm), and the total intensity ratio is $I_\infty/I_d = 0.8$, where the two input beams are of equal intensity. When one of the dark beams is turned off (for the same other parameters), each beam does not maintain a constant width while propagating. Instead, it diffracts to 21 μm, as illustrated in Fig. 6(b) and Fig. 6(c). These results agree well with experimental results of Fig. 5. We note that in our experiment with a coupled dark–dark soliton pair, the bias field used is somewhat higher than that predicted from theory. We attribute this to two reasons: One is the residual grayness in the dark solitons. Because the step mirrors used in experiments do not provide an ideal π phase jump in the wave fronts of the dark beams, dark solitons are formed with some grayness. The other reason is partial guidance of the background beam under the dark soliton, i.e., guidance by the waveguide induced by the soliton. This latter effect modulates the background illumination locally so that it is no longer uniform, as assumed in the theory.[5,19,20]

As expected, the decoupling behavior becomes less pronounced as we reduce (or eliminate) the background illumination and work in the region of high intensity ratio ($I_\infty/I_d \gg 1$). When we set the total intensity of the dark beams much higher than the effective dark irradiance (e.g., remove the background illumination and use the natural dark irradiance in the crystal, thus $I_\infty \gg I_d$), we observe that two beams couple to a dark–dark soliton pair by applying a lower voltage (in accordance with the existence curve for dark solitons), but we cannot observe any change on either one of the beams after its mate is blocked. From the soliton existence curve of Fig. 1(b) this corresponds to moving the operating point on the far

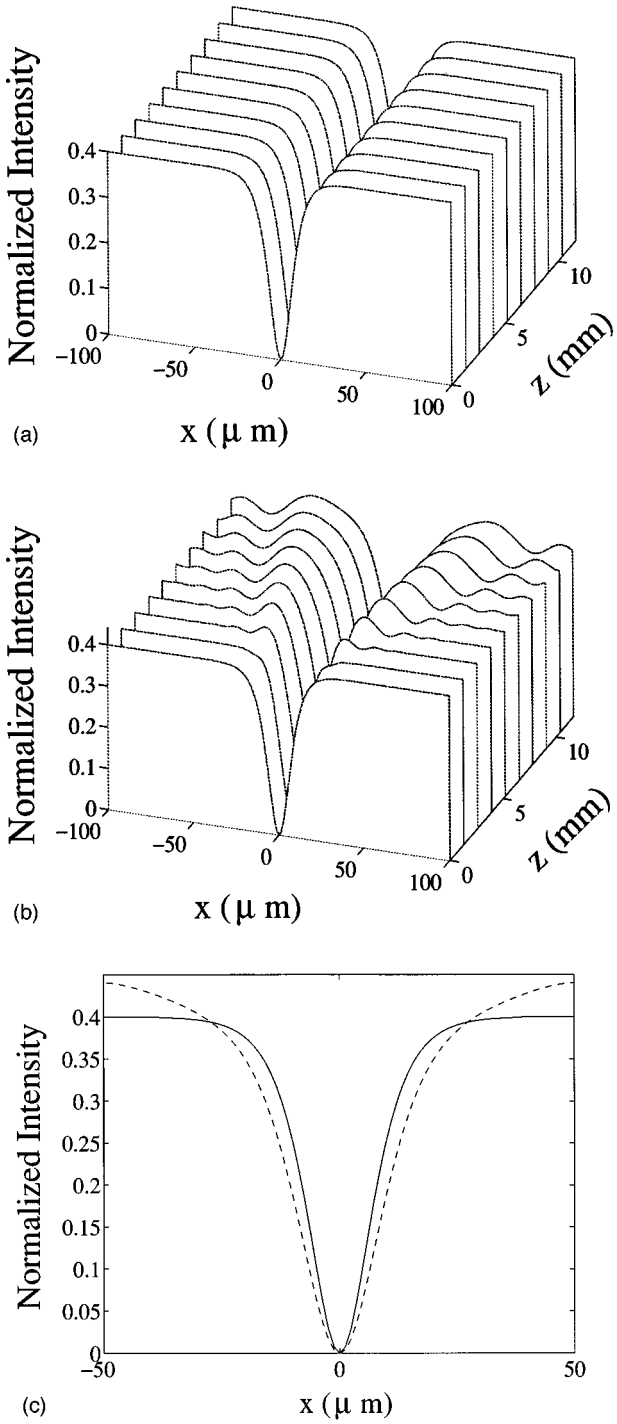

Fig. 6. Numerical simulations corresponding to Figs. 5(c) and 5(d): (a) propagation of one of the dark beams from a coupled dark–dark soliton pair; (b) propagation of one of the dark beams when the pairing beam is absent, and (c) input (solid) and output (dashed) intensity profiles corresponding to (b).

right side of the curve, which is nearly a flat line. Therefore, as one component is blocked, the remaining component still sits on the curve and forms a dark soliton. This robustness of the dark-soliton pair in the region of high-intensity ratio is also found in our numerical simulations, which confirms that the coupled dark-soliton pair is not affected by the decoupling at $I_\infty/I_d \gg 1$.

8. DARK–BRIGHT PAIRS

The experiments with dark–bright pairs are performed in the same crystal as used for bright–bright pairs (codoped SBN:61). The peak intensity of the dark beam (I_∞) is made slightly larger than that of the bright beam (I_0), resulting in a small dip (~36-μm FWHM) in the combined intensity ($I_\infty/I_d = 1.197$, $I_0/I_d = 1.088$). The width of the dark notch is 14 μm, and that of the bright beam is 11 μm (Fig. 7). In the absence of an external field, each beam diffracts while propagating through the crystal. By applying a (negative) voltage of 400 V between the two electrodes, we observe that the output beams are coupled into a steady-state fundamental dark–bright soliton pair. Two beams are monitored separately by the same method explained earlier. Figure 7(c) shows photographs of the output dark and bright components taken immediately after the pairing beam is blocked. Again, when the two components are decoupled, each remaining beam alone cannot survive as a fundamental soliton. This is shown in Fig. 7(d), where the photographs are taken after the pairing beam is blocked for a time much longer than the crystal response time and a single-beam steady state is established. Since the polarity of the applied voltage is not appropriate for the bright soliton, the bright beam alone diffracts and experiences self-defocusing. In the case of a dark beam alone, since the effective intensity ratio is increased and the voltage is not adjusted, the nonlinearity becomes too high to maintain the fundamental dark soliton. Instead, the dark beam evolves into a triple-soliton structure when the bright beam is absent, and all other conditions are unchanged. Interestingly enough, as we unblock the bright beam after the triple dark-soliton structure is formed (a steady-state is established), we observe first the guidance of the bright beam into the triple-channel waveguide induced by the multiple dark soliton[26] and then the time evolution and reestablishment of a single-channel coupled dark–bright soliton pair toward steady state.[41]

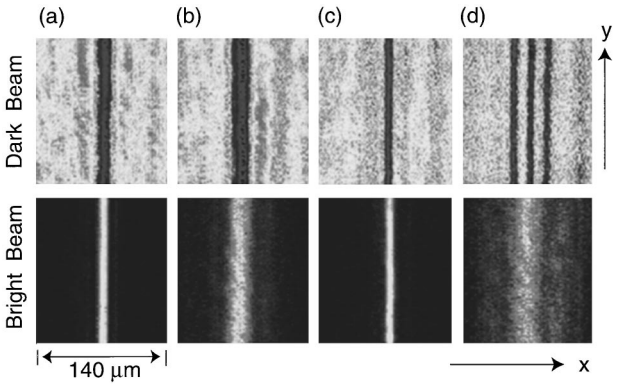

Fig. 7. Experimental results showing coupling–decoupling of a dark–bright soliton pair. Photographs are taken at (a) the input and (b)–(d) the output faces of the crystal: (b) diffraction output from the crystal, (c) coupled output when the pairing beam is present, and (d) decoupled output when the pairing beam is absent.

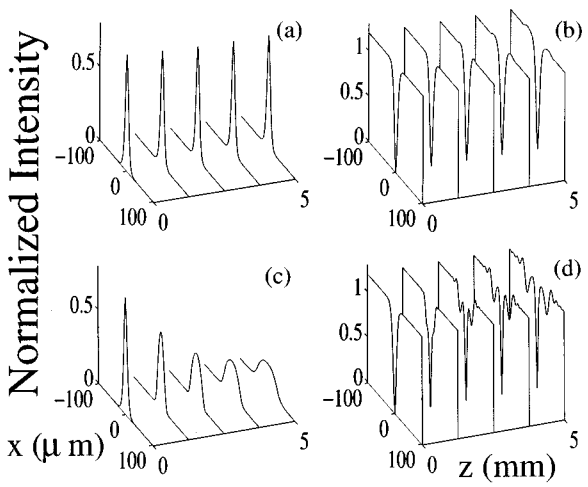

Fig. 8. Numerical simulations corresponding to Figs. 7(c) and 7(d): (a), (b) propagation of the bright and dark components of a coupled soliton pair; (c), (d) corresponding propagation when the pairing component is absent.

The numerical simulations of coupled dark–bright pairs are shown in Fig. 8. The parameters used are close to those of the experiment. The input intensity FWHM of both the bright beam and the dark notch are 14 mm. A bright–dark pair solution is found at $I_\infty/I_d = 1.2$, $I_0/I_d = 0.8$, and a negative voltage $V = -400$ volts (over 4.5 mm). Figure 8 depicts the intensity profiles of the bright–dark components when they propagate in the crystal as a coupled pair. When the pairing beam is absent, the bright beam self-defocuses [Fig. 8(c)], while the dark component evolves into a dark triplet [Fig. 8(d)]. This agrees very well with experimental observations.

9. DISCUSSION

Several issues merit further discussion. The first is the longitudinal stability properties of these photorefractive soliton pairs. Experimentally, we find that both bright–bright and dark–dark pairs are stable against small perturbations such as slight displacement. These soliton pairs exhibit properties similar to those of a steady-state photorefractive screening soliton; thus they are stable just like a single steady-state bright[24] or dark[25] screening soliton. Numerically, this is investigated by beam propagation methods, and it is also found that the bright–bright and dark–dark pairs are stable even if the intensity or width of one of the components is perturbed up to 20%. Figure 9 shows examples for a stable bright–bright (a) and a stable dark–dark (b) pair, where the intensity of one dark beam is perturbed by 20%. However, for the case of dark–bright pairs we find in both experiments and simulations that they are stable only for negative bias but not for positive bias. As an example, we set the peak intensity of the bright beam higher than that of the dark beam ($I_\infty/I_0 \approx 0.8$), obtaining a small peak in the total

intensity, and we use a positive bias field so that it favors trapping of bright solitons.[5,37] The two beams are unstable, and we cannot generate a coupled soliton pair by adjusting the applied voltage. Figure 10 shows a typical example for an unstable dark–bright pair obtained from experiments. Numerical simulations of this case are shown in Fig. 11, obtained at parameters of $I_\infty/I_0 = 0.8$ and $V = +400$ volts. In the range of positive bias fields that we used, each component of the pair suffers from modulation instability.

Transverse instability is the second issue. In all experiments described here, we observe that the coupled pairs are stable against transverse modulation instability. Although it is commonly accepted that *any* (1 + 1)-dimensional beams propagating in a three-dimensional (bulk) medium should be transversely unstable,[56] from all our experiments with photorefractive solitons it is apparent that as long as the parameters of the beam and nonlinearity are on or close to the existence curve, the transverse modulation instability is arrested to a certain degree that it is *not* observed even within a propagation length of 1 cm or longer (see Fig. 5). However, if the parameters deviate considerably from the existence curve, transverse instabilities become dominant for either bright or dark solitons, single beams, or coupled pairs.[24,39] In fact, this is what happens to the decoupled bright–bright soliton pair: as one component is blocked, the remaining component is severely distorted by the transverse modulation instability. Based on our observations, we conjecture that, for all (1 + 1)-dimensional solitons propagating in a three-dimensional (bulk) *saturable* nonlinear medium, transverse instabilities are arrested when (a) the beam parameters correspond to points on the existence curve (i.e., a soliton forms), and (b) the soliton is in the saturated intensity regime. Obviously, it is very interesting to investigate theoretically and experimentally the transverse stability properties of photorefractive solitons and soliton pairs. We leave these issues for future studies.

Third, we would like to elaborate on the master–slave relation between coupled solitons. In both cases of bright–bright and dark–dark pairs we observe the master–slave relation when the intensity of one component is much higher than that of the other. For bright–

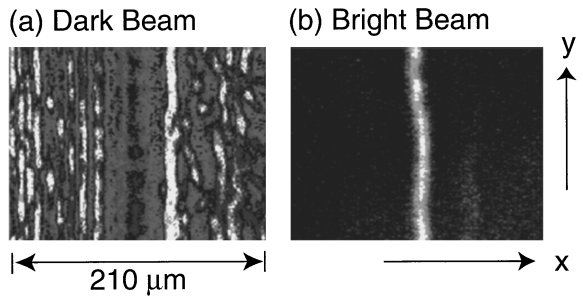

Fig. 10. Experimental results showing output (a) dark and (b) bright components from an unstable dark–bright pair.

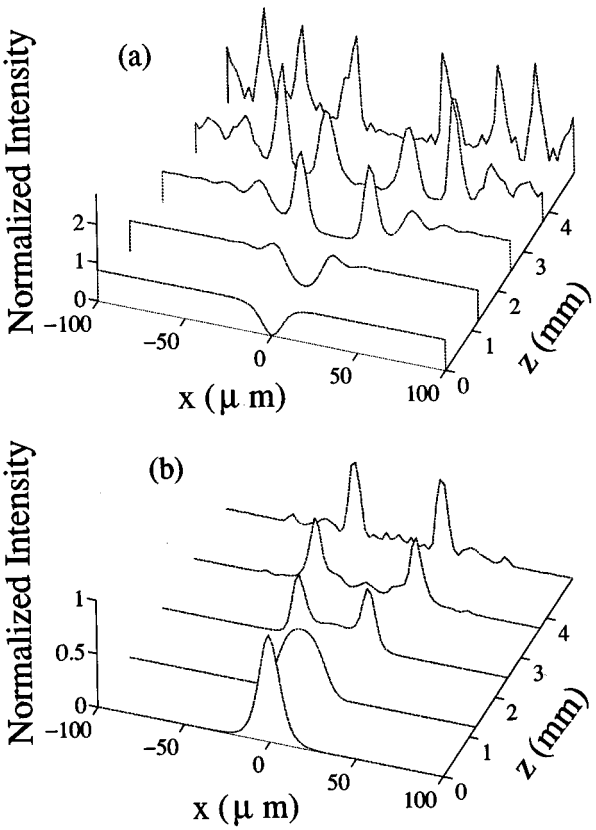

Fig. 11. Numerical simulations showing unstable propagation of a dark–bright pair corresponding to Fig. 10: (a) the dark component and (b) the bright component.

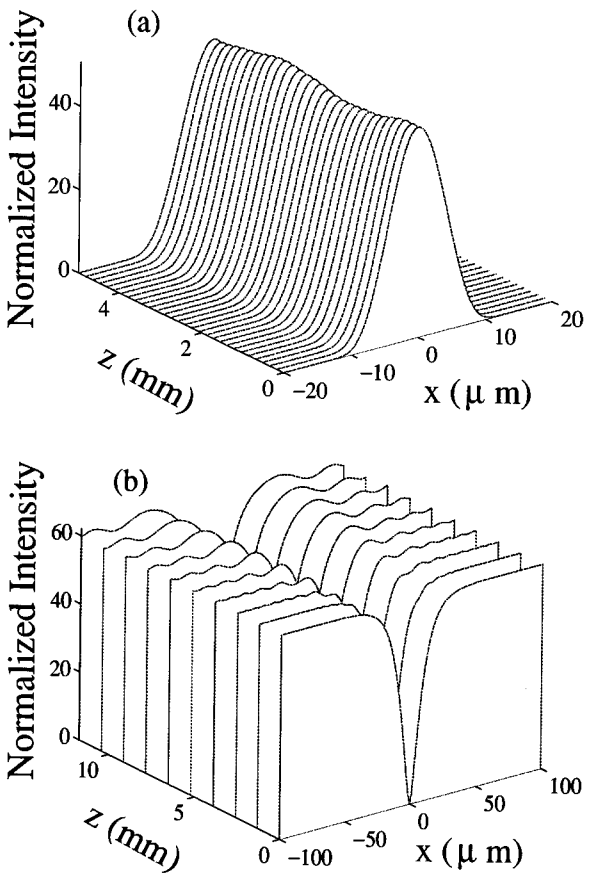

Fig. 9. Numerical simulations showing stable propagation of (a) a bright–bright and (b) a dark–dark soliton pair when the intensity of one of the components is perturbed by 20% at the input.

bright pairs, when one beam is much stronger than the other, mutual self-trapping is observed at proper conditions. But removing the weak beam does not affect the strong beam (the strong beam alone remains to be a soliton), whereas removing the strong beam does affect the weak beam (the weak beam alone cannot remain as a soliton). Since the waveguide is mainly created by the strong beam, it cannot be sustained after the strong beam is removed, and thus the weak beam is distorted because of the high bias field. For dark–dark pairs, similar behavior is observed in the region of low intensity ratio (i.e., when the combined intensity of the two beams is lower than the effective dark irradiance); removing the weak beam does not affect the strong beam, whereas removing the strong beam causes broadening of the dark notch borne in the weak beam. In this case the refractive-index modulation is dominated by the strong beam. Once it is removed, the weak one diffracts. Experimental results and numerical simulations of this case for a dark–dark pair are shown in Fig. 12 and Fig. 13, respectively, where the intensity of the strong beam is approximately 15 times higher than that of the weak beam. For the dark–bright case, coupled soliton pairs are obtained only when their peak intensities are nearly equal. When the bright beam is too weak compared with the dark one, we observe a master–slave relation. The bright beam is guided in the dark soliton-induced waveguide, but it does not affect the dark soliton; i.e., nothing happens to the dark soliton when the bright component is removed. This master–slave relation is directly related to the optical guiding properties of waveguides induced by screening solitons, as the weak component is guided by the waveguide induced by the strong component.

Finally, we want to point out that the observed spatial soliton pairs are actually analogous to vector solitons[57–59] involving two optical beams with orthogonal polarizations, and in particular, to the Manakov solitons[50] discussed in Section 4. It is also worth noting that all our experiments with photorefractive spatial soliton pairs are performed with low-power cw laser beams, whereas previous experiments with spatial soliton pairs[13] or Manakov spatial solitons[51] had to use high-power laser pulses.

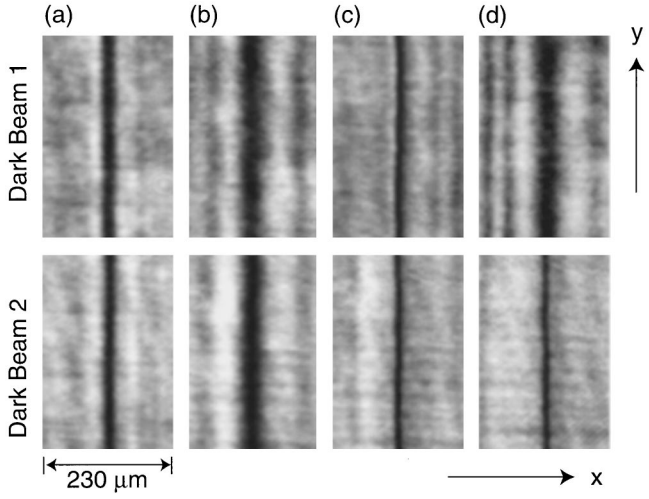

Fig. 12. Experimental results showing the master–slave relation in a dark–dark pair when the intensity of one of the components is much higher than that of the other. Photographs are taken at (a) the input and (b)–(d) the output faces of the crystal: (b) diffraction output, (c) output when both beams are present, and (d) output when the other beam is absent. Beam 1 is the weak beam, and beam 2 is the strong beam.

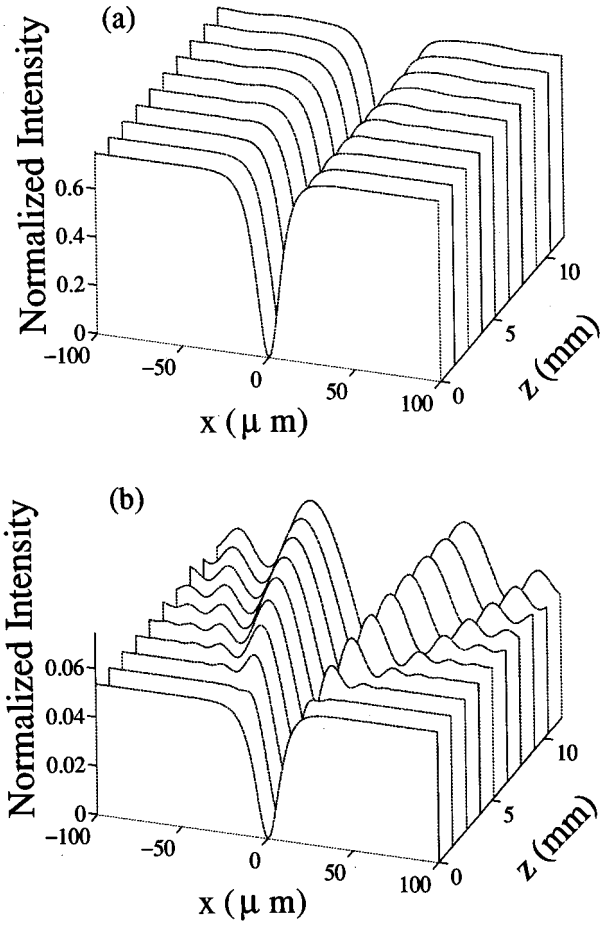

Fig. 13. Numerical simulations corresponding to Fig. 12(d). Shown are (a) the strong beam and (b) the weak beam after removing the pairing beam.

10. CONCLUSION

We have presented a comprehensive experimental and theoretical study on incoherently coupled photorefractive spatial soliton pairs, including all three different realizations: bright–bright, dark–dark, and dark–bright. These soliton pairs involve two steady-state photorefractive screening solitons coupled to each other through their nonlinear intensity superposition, which can be understood intuitively from the standpoint of the soliton existence curve. We show that, in general, a coupled photorefractive soliton pair is analogous to Manakov solitons, in which both beams are mutually trapped and cannot survive as solitons after decoupling.

Our study can be further extended in several directions. First, the system of two incoherently coupled equations (4) may possess more general solutions for coupled solitary waves, e.g, those with different widths of the coupled solitons. Such localized solutions are not possible in the limit of Manakov solitons,[50] even for the case of dark-bright soliton pairs.[53] However, we expect

that nonintegrability of the system may bring some new features in the structure of the incoherently coupled solitons. Second, the stability of the incoherently coupled solitons described by the system [Eqs. (4)] is still an open problem. Finally, it is also important to study different types of interactions between the soliton coupled states. For instance, as was recently mentioned,[60] the interaction of coupled dark–bright soliton pairs can differ drastically from the interaction of uncoupled solitons.

ACKNOWLEDGMENTS

This research was supported by the U.S. National Science Foundation and the U.S. Army Research Office. We are grateful for assistance from M. Shih and M. Mitchell at Princeton University. Yu. Kivshar is a member of the Australian Photonics Cooperative Research Centre.

REFERENCES AND NOTES

1. R. Y. Chiao, E. Garmire, and C. H. Townes, Phys. Rev. Lett. **13**, 479 (1964).
2. M. Segev, B. Crosignani, A. Yariv, and B. Fischer, Phys. Rev. Lett. **68**, 923 (1992).
3. W. E. Torruellas, Z. Wang, D. J. Hagan, E. W. Van Stryland, G. I. Stegeman, L. Torner, and C. R. Menyuk, Phys. Rev. Lett. **74**, 5036 (1995).
4. V. Tikhonenko, J. Christou, and B. Luther-Davies, Phys. Rev. Lett. **76**, 2698 (1996).
5. M. Segev, M. Shih, and G. C. Valley, J. Opt. Soc. Am. B **13**, 706 (1996).
6. Y. Kivshar, IEEE J. Quantum Electron. **29**, 250 (1993).
7. A. W. Snyder, D. J. Mitchell, and Y. S. Kivshar, Mod. Phys. Lett. B **9**, 1479 (1995).
8. S. Trillo, S. Wabnitz, E. M. Wright, and G. I. Stegeman, Opt. Lett. **13**, 871 (1988).
9. D. N. Christodoulides, Phys. Lett. A **132**, 451 (1988).
10. V. V. Afanasjev, Y. Kivshar, V. V. Konotop, and V. N. Serkin, Opt. Lett. **14**, 805 (1989).
11. V. E. Zakharov and A. B. Shabat, Sov. Phys. JETP **34**, 62 (1972).
12. R. De La Fuente and A. Barthelemy, Opt. Commun. **88**, 419 (1992).
13. M. Shalaby and A. J. Barthelemy, IEEE J. Quantum Electron. **28**, 2736 (1992).
14. R. De La Fuente, A. Barthelemy, and C. Froehly, Opt. Lett. **16**, 793 (1991).
15. G. Duree, J. L. Shultz, G. Salamo, M. Segev, A. Yariv, B. Crosignani, P. DiPorto, E. Sharp, and R. Neurgaonkar, Phys. Rev. Lett. **71**, 533 (1993).
16. M. Morin, G. Duree, G. Salamo, and M. Segev, Opt. Lett. **20**, 2066 (1995).
17. G. Duree, M. Morin, G. Salamo, M. Segev, A. Yariv, B. Crosignani, P. DiPorto, and E. Sharp, Phys. Rev. Lett. **74**, 1978 (1995).
18. N. Fressengeas, J. Maufoy, and G. Kugel, Phys. Rev. E **54**, 6866 (1996).
19. M. Segev, G. C. Valley, B. Crosignani, P. DiPorto, and A. Yariv, Phys. Rev. Lett. **73**, 3211 (1994).
20. D. N. Christodoulides and M. I. Carvalho, J. Opt. Soc. Am. B **12**, 1628 (1995).
21. Steady-state self-focusing in biased photorefractive media was first observed by M. D. Iturbe-Castillo, P. A. Marquez-Aguilar, J. J. Sánchez-Mondragón, S. I. Stepanov, and V. A. Vysloukh, Appl. Phys. Lett. **64**, 408 (1994).
22. Steady-state screening solitons in biased photorefractive media was first observed by M. Shih, M. Segev, G. C. Valley, G. Salamo, B. Crosignani, and P. DiPorto, Electron. Lett. **31**, 826 (1995).
23. M. Shih, P. Leach, M. Segev, M. Garrett, G. Salamo, and G. C. Valley, Opt. Lett. **21**, R324 (1996).
24. K. Kos, H. Ming, G. Salamo, M. Shih, M. Segev, and G. C. Valley, Phys. Rev. E **53**, R4330 (1996).
25. Z. Chen, M. Mitchell, M. Shih, M. Segev, M. Garrett, and G. C. Valley, Opt. Lett. **21**, 629 (1996).
26. Z. Chen, M. Mitchell, and M. Segev, Opt. Lett. **21**, 716 (1996).
27. Z. Chen, M. Segev, S. R. Singh, T. H. Coskun, and D. N. Christodoulides, J. Opt. Soc. Am. B **14**, 1407 (1997).
28. G. C. Valley, M. Segev, B. Crosignani, A. Yariv, M. M. Fejer, and M. Bashaw, Phys. Rev. A **50**, R4457 (1994).
29. M. Taya, M. Bashaw, M. M. Fejer, M. Segev, and G. C. Valley, Phys. Rev. A **52**, 3095 (1995).
30. M. Taya, M. Bashaw, M. M. Fejer, M. Segev, and G. C. Valley, Opt. Lett. **21**, 943 (1996).
31. M. Segev, G. C. Valley, M. C. Bashaw, M. Taya, and M. M. Fejer, J. Opt. Soc. Am. B **14**, 1772 (1997).
32. Z. Chen, M. Segev, D. W. Wilson, R. E. Muller, and P. D. Maker, Phys. Rev. Lett. **78**, 2948 (1997).
33. M. Chauvet, S. A. Hawkins, G. Salamo, M. Segev, D. F. Bliss, and G. Bryant, Opt. Lett. **21**, 1333 (1996).
34. M. Mitchell, Z. Chen, M. Shih, and M. Segev, Phys. Rev. Lett. **77**, 490 (1996).
35. D. N. Christodoulides, T. H. Coskun, M. Mitchell, and M. Segev, Phys. Rev. Lett. **78**, 646 (1997).
36. M. Shih, M. Segev, and G. Salamo, Opt. Lett. **21**, 931 (1996).
37. D. N. Christodoulides, S. R. Singh, M. I. Carvalho, and M. Segev, Appl. Phys. Lett. **68**, 1763 (1996).
38. W. Krolikowski, N. Akhmediev, and B. Luther-Davies, Opt. Lett. **21**, 782 (1996).
39. Z. Chen, M. Segev, T. H. Coskun, and D. N. Christodoulides, Opt. Lett. **21**, 1436 (1996).
40. M. Shih and M. Segev, Opt. Lett. **21**, 1538 (1996).
41. Z. Chen, M. Segev, T. H. Coskun, D. N. Christodoulides, Y. S. Kivshar, and V. V. Afanasjev, Opt. Lett. **21**, 1821 (1996).
42. M. Shih, Z. Chen, M. Segev, T. H. Coskun, and D. N. Christodoulides, Appl. Phys. Lett. **69**, 4151 (1996).
43. G. S. Carcia-Quirino, M. D. Iturbe-Castillo, V. A. Vysloukh, J. J. Sánchez-Mondragón, S. I. Stepanov, G. Lugo-Martinez, and G. E. Torres-Cisneros, Opt. Lett. **22**, 154 (1997).
44. W. Krolikowski and S. Holmstrom, Opt. Lett. **22**, 369 (1997).
45. H. Meng, G. Salamo, M. Shih, and M. Segev, Opt. Lett. **22**, 448 (1997).
46. M. Shih, M. Segev, and G. Salamo, Phys. Rev. Lett. **78**, 2551 (1997).
47. S. R. Singh and D. N. Christodoulides, Opt. Commun. **118**, 569 (1995).
48. W. Krolikowski, N. Akhmediev, B. Luther-Davies, and M. Cronin-Golomb, Phys. Rev. E **54**, 5761 (1996).
49. J. S. Aitchison, A. M. Weiner, Y. Silberberg, D. E. Leaird, M. K. Oliver, J. L. Jackel, and P. W. Smith, Opt. Lett. **16**, 15 (1991).
50. S. V. Manakov, Sov. Phys. JETP **38**, 248 (1974).
51. J. U. Kang, G. I. Stegeman, J. S. Aitchison, and N. Akhmediev, Phys. Rev. Lett. **76**, 3699 (1996).
52. R. Radhakrishnan and M. Lakshmanan, J. Phys. A **28**, 2683 (1995).
53. A. P. Sheppard and Y. S. Kivshar, Phys. Rev. E **55**, 4773 (1997).
54. M. I. Carvalho, S. R. Singh, and D. N. Christodoulides, Opt. Commun. **120**, 311 (1995).
55. S. R. Singh, M. I. Carvalho, and D. N. Christodoulides, Opt. Commun. **130**, 288 (1996).
56. V. E. Zakharov and Rubenchik, Sov. Phys. JETP **38**, 494 (1974).
57. M. Segev, G. C. Valley, S. R. Singh, M. I. Carvalho, and D. N. Christodoulides, Opt. Lett. **20**, 1764 (1995).
58. S. R. Singh, M. I. Carvalho, and D. N. Christodoulides, Opt. Lett. **20**, 2177 (1995).
59. M. I. Carvalho, S. R. Singh, D. N. Christodoulides, and R. I. Joseph, Phys. Rev. E **53**, R53 (1996).
60. A. P. Sheppard and Y. S. Kivshar, in *Nonlinear Guided Waves and Their Applications*, Vol. 15 of 1996 OSA Technical Digest Series (Optical Society of America, Washington, D.C., 1996), p. 157.